International Journal of Power Electronics and Drive System (IJPEDS)
Vol. 8, No. 2, June 2017, pp. 534~547
ISSN: 2088-8694, DOI: 10.11591/ijpeds.v8i2.pp534-547

FOC of SRM using More Efficient DC-DC Converter Topology

Emad S. Abdel-Aliem
Departement of Electrical Engineering, Shoubra Faculty of Engineering, Benha University, Egypt

Article Info

Article history:

Received Feb 16, 2017
Revised Apr 16, 2017
Accepted May 1, 2017

Keyword:

Advance turn-on
Angle control
FOC
Retard/Delay turn-off
SRM

ABSTRACT

Numerous studies had been made to improve the switched reluctance motor operation depend on the modification of the machine design, proposing the converter designs and/or applying a suitable control method. This paper introduces the field orientation control method for that motor using a simple and very efficient DC-DC converter topology. This control method is presented by two techniques; first technique is the advance of the turn-on switching angle and the other technique is the retard/delay of the turn-off switching angle. Instantaneous and average motor characteristics are obtained using Matlab/Simulink software package. Comparison between the simulation results presented using two converter types. A precise speed and torque control are obtained. The average total torque per current is maximized.

Corresponding Author:

Emad S. Abdel-Aliem,
Department of Electrical Engineering,
Shoubra Faculty of Engineering,
Benha University, 108 Shoubra Street, Cairo, Postal code: 11241, Egypt.
Email: emad.sami@feng.bu.edu.eg

1. INTRODUCTION

The switched reluctance motor (SRM) is being used in various number of applications because of it has many merits over the other motor types. The SRM has a simple and robust construction. However, it basically generates large torque ripples compared with the other types of brushless DC motors. For that reason, to improve its operation and reducing the torque ripples, a development in its converter construction and/or a best control strategy is used [1]-[6], [37]-[38].

One of the main approaches of the research in SRM drives is the converter design. The operation and the cost of SRM drive system is mainly affected by the performance of the motor converter [7,8]. Many converter topologies have emerged through continued researches by reducing the number of switches in the converter and also getting faster switch commutation time [3,9-10]. This leads to a simple drive system and enables significant energy savings [11]-[14]. A high performance SRM drive is mainly characterized by minimization of the torque ripples and maximization of the motor efficiency and the torque per current [6],[15]. This criterion can be realized by optimizing the control parameters of the motor such as supply voltage, current level, turn-on, turn-off and the dwell angle [16]-[20].

A closed loop control with a simple DC-DC converter construction [21] for a 3-phase 6/4 SRM with Field Orientation Control (FOC) (known as some times; the switching angle control) method is introduced in this research to get the most efficient operation over the entire range operation of the SRM.

The complete block control diagram for a 3-ph 6/4 SRM drive system using FOC is shown in Figure 1. A standard DC source of 220V is used with the 3-ph DC-DC converter. The speed sensor is an integral part of the SRM drive system, may be optical encoders, resolver or hall-effect sensor [22]-[24] is mounted on the motor shaft to determine the actual rotor speed. A speed-angle converter can used to convert the measured speed into actual measured angle (θ_m) for comparison with the turn-on (θ_{on}) angle and the turn-off (θ_{off}) angle to excite and commutate the phase windings. A digital controller named as a switching angle controller [25] is used to synchronize the switching angles with their respective positions. This angle controller regulates the angles at which excitation of motor phases is achieved. So, it allows the rotor to continuously rotate, producing torque in accordance with the load being applied. The gate drive circuit (triggering circuit) contains integrated circuit components must be used between the angle controller and the power converter. The control logic signals are too small to drive the power switches of the converter. So, the gate drive circuit is used to amplify the control logic signals to the value of current levels required for switching the power converter, and also acts as a good isolation circuit (because it contains opto-coupler) between controller circuit and converter [26].

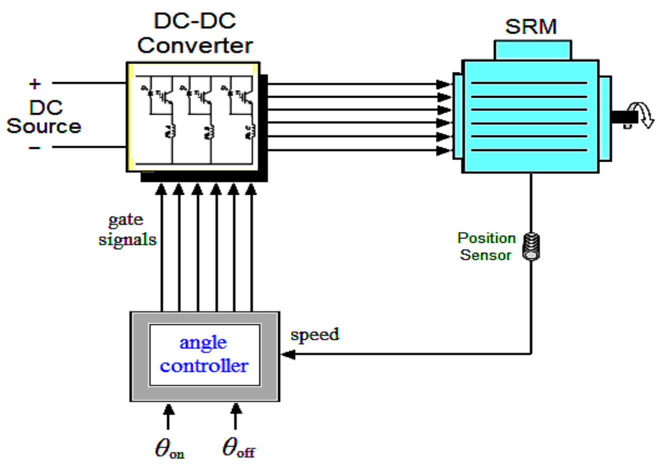

Figure 1. Main components of SRM drive system

This research is organized as follows. The operation of SRM and its mathematical model are reviewed in Section 2. DC-DC converter topology is presented in Section 3. Simulation results using FOC are illustrated in Section 4. The research conclusions are given in Section 5.

2. OPERATION AND MATHEMATICAL MODEL OF SRM

Due to the advances in power electronics, sensors and controllers in the recent years, the SRM has gained a great of commercial and industrial interest [27]. It has a simple and robust construction due to the magnetic circuitry of the motor neither requires permanent magnets nor windings in the rotor. The stator has concentrated coils around the poles that are excited sequentially through DC voltage pulses. The motor has salient poles on the stator and also on the rotor, so, it is named as a doubly salient pole machine [27,28]. The term "switched reluctance" tends to that the reluctance of the machine is switched. The term magnetic "reluctance" depends on the rotor position and the term "switched" refers to the electronic commutation of the electrical phases by means of a power electronics converter [28].

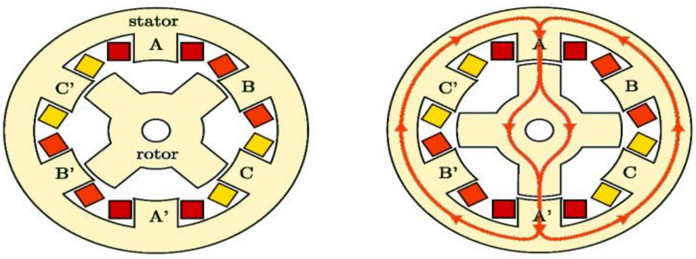

(a) unaligned position (b) aligned position

Figure 2. Unaligned and aligned positions for phase-A of a 3-phase 6/4 SRM

The SRM torque production is based purely on the variation of the magnetic reluctance. The magnetic circuits of the motor are symmetrical and have almost zero mutual flux linkages among stator windings even under saturated conditions. The self inductance of the phase windings only is responsible for production of torque [28]. Figure 2 shows a typical three-phase machine configuration, N_{ph} = 3. The machine has six stator poles N_s= 6 and four rotor poles N_R = 4, this configuration is known as a 6/4 SRM. From a magnetic perspective, each phase of the 6/4 machine has two magnetic poles per phase, *i.e.*, one pole pair, given that diametrically opposed coils are electrically connected in series or in parallel. For example, the phase A is made up of concentrated coils on poles A and A'. The rotor position shown in Figure 2a is called the unaligned position with respect to phase A–A', this unaligned position for the phase A is the position of the largest magnetic reluctnace between stator and rotor poles. If the phase A is excited, a magnetic flux path is formed by the two stator pole A–A', as in Figure 2b, which is the position of the smallest magnetic reluctance [29]. The complete mathematical model of the SRM in [21] is a set of differential equations which are obtained using standard electromagnetic theory. These differential equations are as follows:

$$U_j = i_j R_j + \frac{d\lambda_j(i_j,\theta)}{d\theta} \tag{1}$$

Where U_j denotes the phase voltage, i_j denotes the phase current, R_j denotes the phase resistance, j is the active phase, and λ_j (i_j,θ) is the flux linkage. Equation (1) can be rewritten as:

$$U_j = i_j R_j + \frac{\partial\lambda_j(i_j,\theta)}{\partial i}\frac{di_j}{dt} + \frac{\partial\lambda_j(i_j,\theta)}{\partial\theta}\frac{d\theta}{dt} \tag{2}$$

The flux linkage in an active phase is given by the product of the self-inductance and the instantaneous phase current as follows:

$$\lambda_j(i_j,\theta) = L_j(i_j,\theta)\cdot i_j \tag{3}$$

By substituting from Equation (3) into Equation (2) gives:

$$U_j = i_j R_j + L_{jinc}\cdot\frac{di_j}{dt} + i_j\cdot\frac{\partial L_j(i_j,\theta)}{\partial\theta}\cdot\omega \tag{4}$$

$$= i_j R_j + L_{jinc}\cdot\frac{di_j}{dt} + K_v\cdot\omega \tag{5}$$

$$L_{jinc} = \frac{\partial\lambda_j(i_j,\theta)}{\partial i} = \frac{\partial L_j(i_j,\theta)\cdot i_j}{\partial i} = L_j(i_j,\theta) + i_j\cdot\frac{\partial L_j(i_j,\theta)}{\partial i} \tag{6}$$

$$\omega = \frac{d\theta}{dt} \tag{7}$$

Where L_{jinc} is the phase incremental inductance, K_v is the current-dependent back-emf coefficient, and ω is the rotor angular speed. Rearranging Equation (4) gives:

$$\frac{di_j}{dt} = \frac{1}{L_{jinc}}\left(U_j - i_j R_j - i_j\cdot\frac{\partial L_j(i_j,\theta)}{\partial\theta}\cdot\omega\right) \tag{8}$$

$$J\frac{d^2\theta}{dt^2} = J\frac{d\omega}{dt} = \sum_{J=1}^{K} T_j(i_j,\theta) - B\omega - T_L(\omega) \tag{9}$$

Where J and B are the moment of inertia and the viscous friction coefficient, respectively; and T_L is the load torque. Equations (7), (8) and (9) represent the complete mathematical model of the SRM in the case of non-linear modeling for operation of the motor in a real mode. With the non-linear operation; the shape of the inductance is sinusoidal depends on the rotor position, the phase current, and the motor geometry.

The static SRM characteristics can be represented basically via two methods. The first is to plot the variation of phase inductance with respect to rotor position at different phase currents; this way is used in this research. The second way is to plot the variation of phase flux linkage with rotor position and phase currents.

3. DC-DC CONVERTER TOPOLOGY

The SRM cannot run directly from AC or DC source; unlike induction motors or DC motors. So, a power electronics DC-DC converter must be located between the motor and the source. The purpose of the power converter circuit is to provide an increasing and decreasing the current supplied to the phase winding in order to produce a continuous motion [28]. In the feedback path between the motor and the power converter, a control circuit is used to monitor the current and the position feedback in order to produce the correct switching signals for the power converter for matching the demands placed on the drive by the user.

Since the torque developed by the SRM not depends on the current polarity, the motor can operate based on the principle of unipolar current. The current therefore can be supplied to the phase winding with only one switch per phase connected in series with the winding, as shown in Figure 3 [21]. By turning on and off this switch; the flow of the phases current can be regulated. The best feature for that converter is that each phase contains only one switch. This converter topology can be used with a three phases SRM and can be simply modified to suit another type of SRM has different number of phases. Since the mutual coupling between phases is almost negligible, the stored magnetic field energy can create problem during commutation of the phase. The stored magnetic field energy has to be provided a path during commutation (as shown in Figure 3, a freewheeling diode is used in each phase): otherwise excessive voltage can develop across the winding and may result in failure of the semiconductor switch that connected in series with the phase winding [30]-[32].

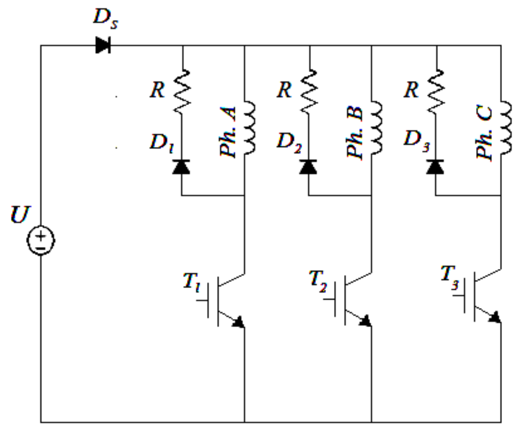

Figure 3. Simple DC-DC converter for 3-phase, 6/4 SRM

As shown in Figure 3, the power switches can be protected using RC snubber circuit. This snubber circuit protects the switch from a large *di/dt* during turn-on and large *dv/dt* during turn-off. Also the snubber circuit provides an effective means of transferring the switching losses from the switch to the snubber resistor, leading to a lower junction temperature rise and better thermal management for the switch and also the no recover of energy to DC source not cause reduction of the overall efficiency of the drive drive [33]-[34].

The diode D_s is used to safe the DC source from the recover energy of each motor phase. No reduction of the overall efficiency of the motor drive because there is no recover of energy to the DC source. The steady state of motor characteristics is reaches faster than using the traditional DC-DC converters [35]-[36].

4. SIMULATION RESULTS USING FOC

The torque of SRM has a strong pulsations at the commutation intervals because the two adjacent phases produce additive torques. Therefore, the FOC can be used to control the SRM drive. This control strategy is based on controlling the values of the switching angles and the dwell angle. The machine efficiency and the average total torque per current will maximize by using this control strategy. So, the FOC is used to control the dwell angle and the input source voltage instantaneously in order to obtain a precise speed control.

In the real control system, control of the switching angles can be realized by a simple feedback circuit using detecting position sensor on the motor shaft as shown in Figure 4. The switching angle controller in that figure regulates the motor performance via integration of the motor speed to produce the measured position of the rotor by comparing the measured rotor position with the switching angles θ_{on} and θ_{off}. In order to produce the gate signals of the converter switches. A gate drive circuit must be used between the angle controller and the converter, it receives the logic signals that has a low level from the angle controller and transmit these signals but with a high level to the converter. In other means; the gate drive circuit is used to isolate the control circuit from the power circuit.

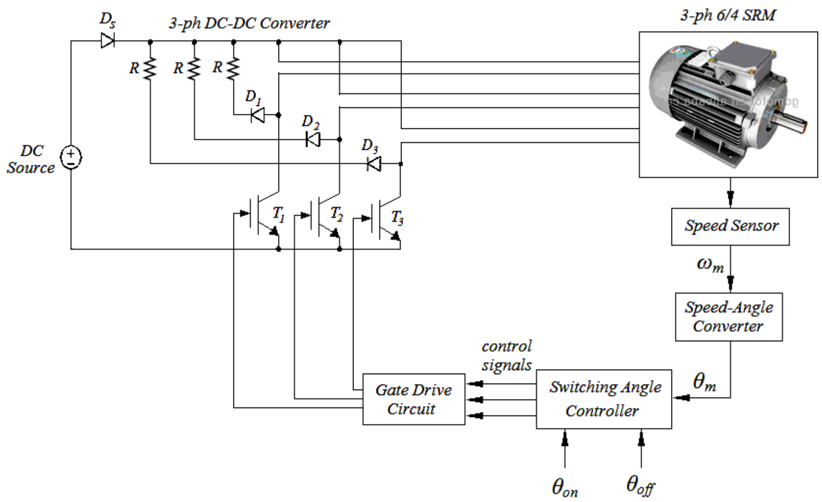

Figure 4. Complete block control diagram for 3-ph 6/4 SRM drive system using Field Orientation Control

The back-emf in the motor becomes significant as the motor speed increases. It is necessary to retard the turn-off angle or advance the turn-on angle in order to reach the reference current before the poles overlap. One reason of the torque ripple is that the negative torque due to the tail current (which will be solved using the FOC method). Also, the decay of current in the demagnetizing case can be enhanced through decaying it in fast time using FOC. In this part, the motor firing/switching angles change by the means of a software to obtain the best values for these angles.

The block control diagram of Figure 4 can be simulated using Matlab/Simulink software package. The data required for that motor drive system obtained from the APPENDIX. The simulation results obtained for no-load, θ_{on} = 40^o, and θ_{off}=70^o.

4.1. Instantaneous Characteristics with Advance Turn-On

The instantaneous phase current versus rotor position is shown in Figure 5. The principle of increasing the advance of the turn-on angle θ_{on} (i.e., decreasing the value of the turn-on angle) is to increase the average motor total torque. The phase current I_A has θ_{on} = 40^o, θ_{off} = 70^o and advance for θ_{on} by a step of 2^o. The phase current I_A has three cases for advance of θ_{on}. The case of the solid line (where, θ_{on} = 40^o) there is no advance for the phase current. The case of the dashed line (where, θ_{on} = 38^o) an advance by 2^o is obtained. The case of the dotted line (where, θ_{on} = 36^o), the phase current has an advance by 4^o. Then, when we see deeply, the phases current increases as the turn-on angle is advanced, also, the motor total current or the source current increases (but this is undesirable) to produce an increase in the average total torque as shown in Figure 5 and Figure 6 respectively.

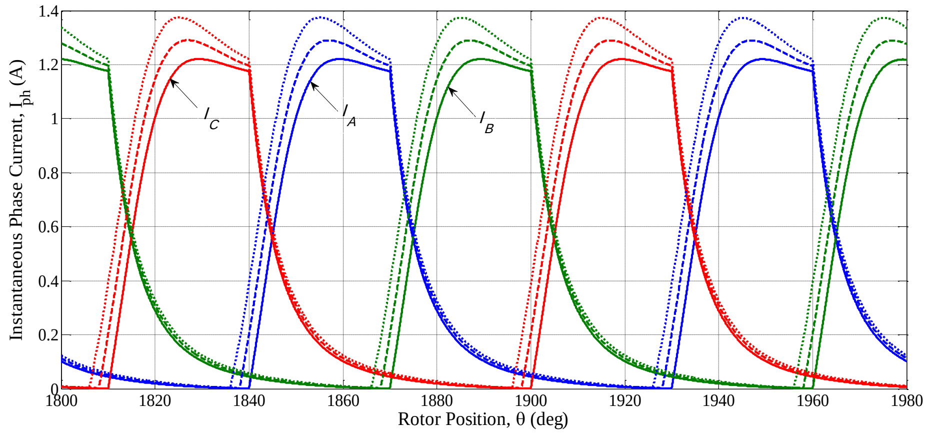

Figure 5. Instantaneous motor phases current versus rotor position for advance turn-on

As shown in Figure 5 the phase current increases with increasing the advance turn-on, because the conduction period of the phase current increases as the advance increases. But, there is a limit of increasing the phase current to be not greater than a maximum allowable range. This maximum allowable current occurs when the source current has the value 1.25 of the rated source current. For that converter design; the average steady state phase current at θ_{on} = 40^o, θ_{off} = 70^o equals to 0.42A, but for the asymmetric bridge at the same switching angles, the average steady state phase current equals 0.9A [35].

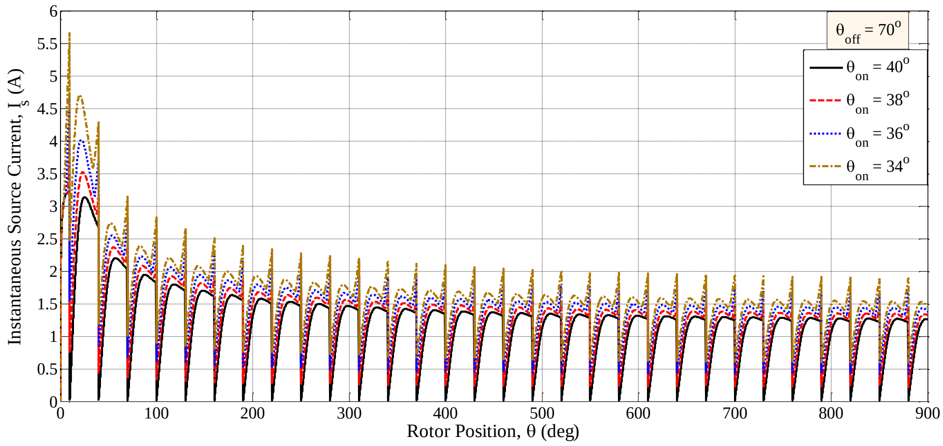

Figure 6. Instantaneous source current versus rotor position for advance turn-on

The instantaneous total torque versus rotor position is shown in Figure 7 the total torque increases as the advance of the turn-on angle increases, also, if there is a negative torque found, the advance can eliminate it. The average total torque at θ_{on} = 40^o and θ_{off} = 70^o equals 4.279Nm but in the asymmetric bridge converter equals 2.160Nm [35].

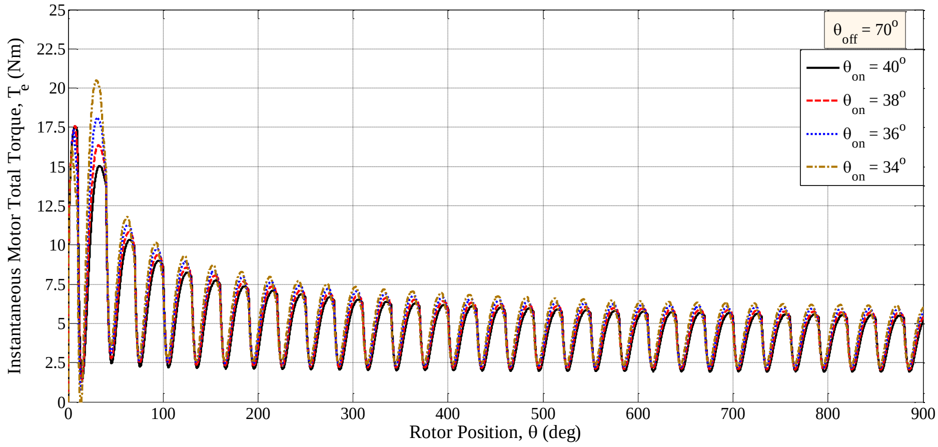

Figure 7. Instantaneous motor total torque versus rotor position for advance turn-on

4.2. Instantaneous Characteristics with Retard Turn-Off

On the other hand, the principle of retarding the turn-off angle (i.e., increasing the value of the turn-off angle θ_{off}) based on increasing the conduction period between the switching angles for increasing the average motor total torque. The instantaneous phase's current versus rotor position for retard the turn-off is shown in Figure 8. The phase current I_A has constant angles θ_{on} = 40^o, θ_{off} = 70^o and retard for θ_{off} by step of 2^o. The phase current I_A has three cases for retad/delay of θ_{off}. The case of solid line there is no delay (where, θ_{off} = 70^o). The case of the dashed line a delay by 2^o (where θ_{off} = 72^o) is obtained. The case of the dotted line (where, θ_{off} = 74^o) the phase current has a delay by 4^o. Then, when we see deeply, the phases current decreases as the turn-off angle is delayed further, also, the motor total current decreases (this is desirable); but the motor total torque decreases as the retarding/delaying of the turn-off angle increases, as shown in Figure 9 and Figure 10 respectively.

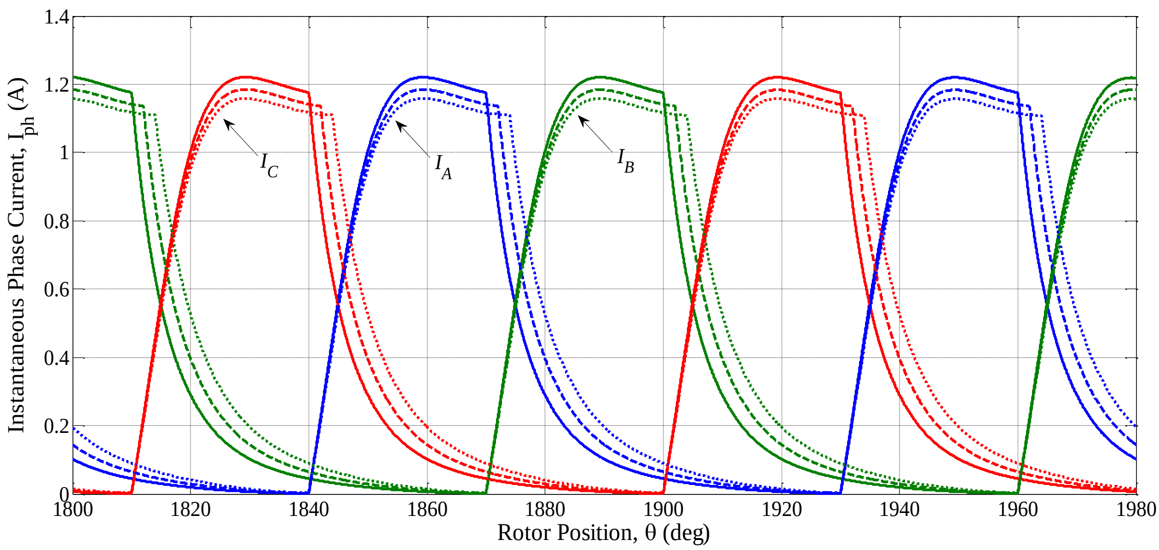

Figure 8. Instantaneous motor phases current versus rotor position for retard turn-off

As shown in Figure 7 and Figure 10; the motor total torque at using the retarding of the turn-off angle has a less negative vaule compared with using advancing of the turn-on angle. Also as shown in Figure 5 and Figure 8; the average value of motor phase current increases as the advance turn-on increases but decreases as the retard of the turn-off increases. Similarly, as presented in Figure 6 and Figure 9 the instantenous source current increases as advance turn-on increases, but decreases as the retard turn-off increases.

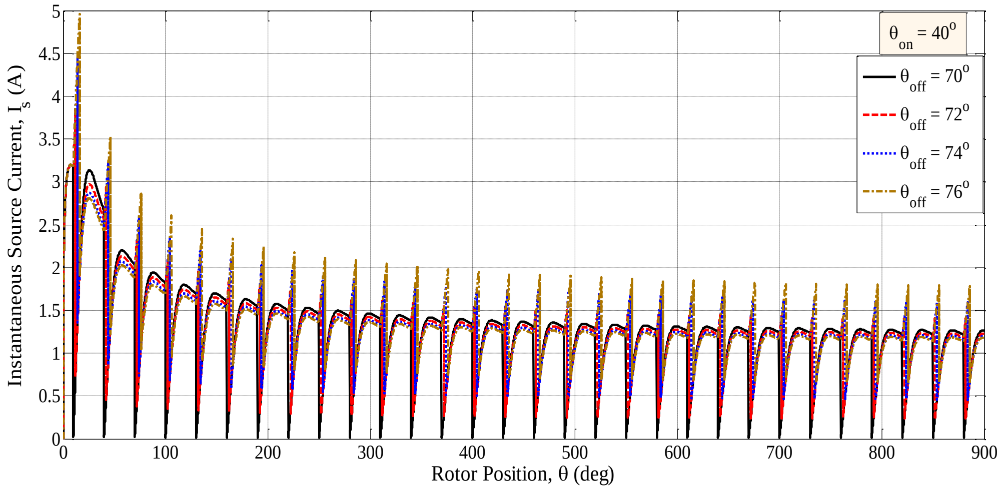

Figure 9. Instantaneous source current versus rotor position for retard turn-off

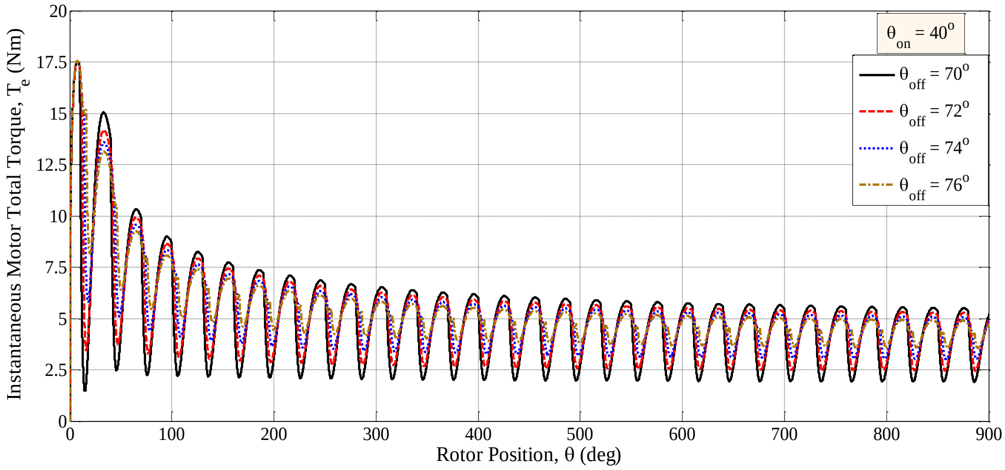

Figure 10. Instantaneous motor total torque versus rotor position for retard turn-off

4.3. Average Characteristics with Advance Turn-On

For easy comparison between motor characteristics at using the advance turn-on and the retard turn-off; the motor average characteristics are introduced. The average source current versus rotor position at using advance turn-on, is shown in Figure 11; at constant the turn-off angle (say θ_{off} = 70^o), as the switching turn-on angle decreases the average source current increases. Also; as shown in Figure 12; at constant turn-off angle (say, θ_{off} = 70^o) as the switching turn-on angle decreases, the average total torque increases. In other words, for constant turn-off angle; the average source current or average total torque increases as the advance of the turn-on angle increases.

From Figure 11 and Figure 12; more advancing of turn-on angle produces large increase in the average source current and a small increase in the average total torque, so, this will lead to decrease in the average total torque per current as presented in Figure 13. Also, as shown in Figure 14, increasing the advance of turn-on angle leads to increases of motor speed.

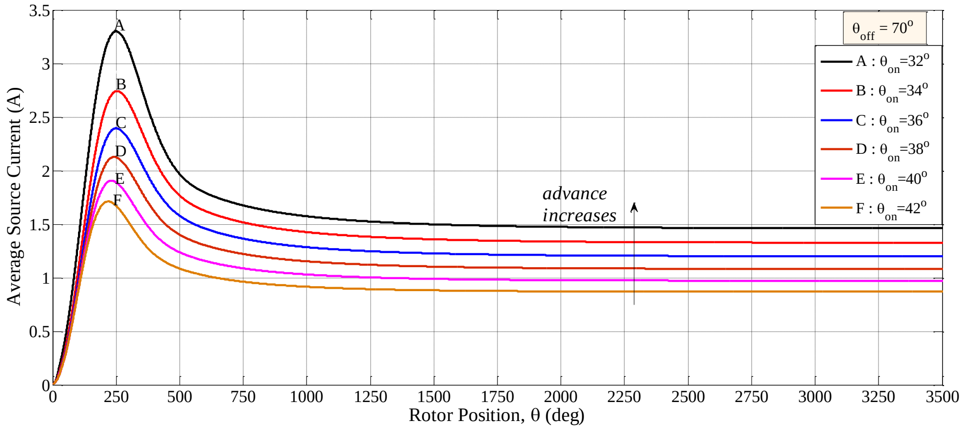

Figure 11. Average source current versus rotor position for advance turn-on

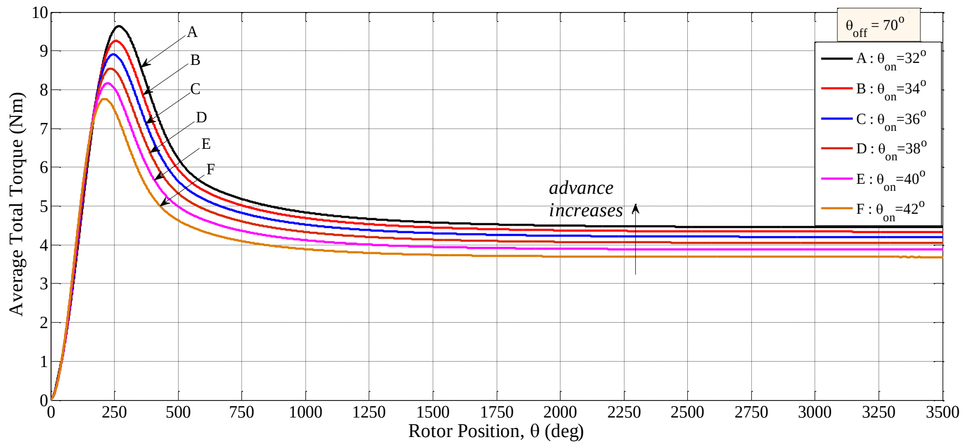

Figure 12. Average total torque versus rotor position for advance turn-on

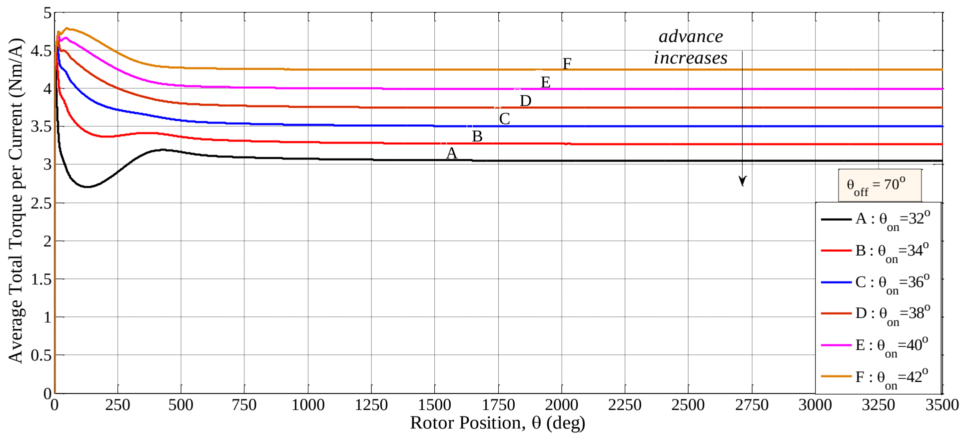

Figure 13. Average total torque per current versus rotor position for advance turn-on

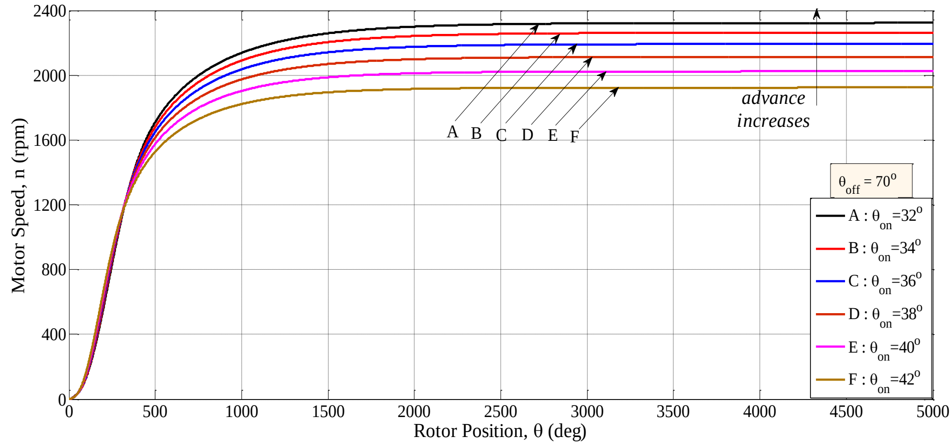

Figure 14. Motor speed versus rotor position for advance turn-on

4.4. Average Characteristics with Retard Turn-Off

After presentation of average characteristics with the change of the rotor position at using advance turn-on angle; the average characteristics for the retard turn-off is presented in this subsection. As shown in Figure 15 for a constant turn-on angle (say, θ_{on} = 40^o), as the value of the turn-off angle increases, the average source current increases. This means that, the average source current increases as the retard of the turn-off angle increases. Similarly, as shown in Figure 16, the average total torque increases as the retard of the turn-off angle increases.

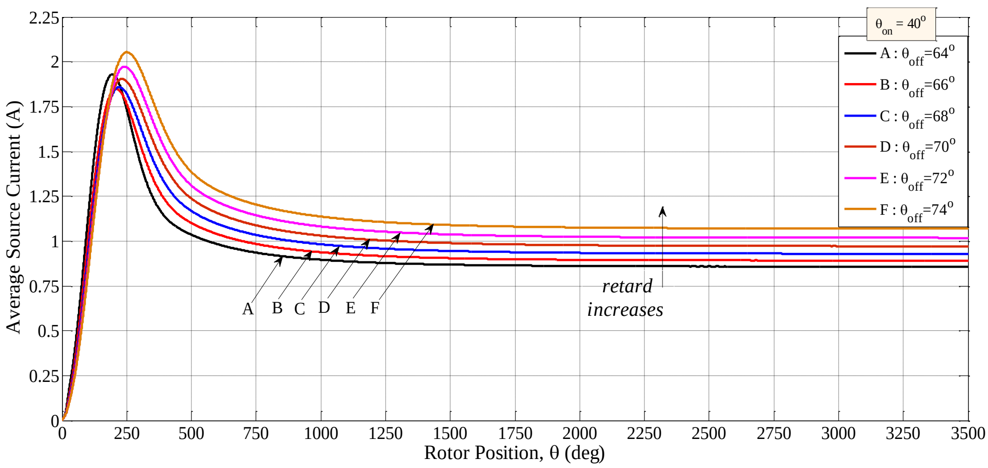

Figure 15. Average source current versus rotor position for retard turn-off

As shown in Figure 17 the average total torque per current versus rotor position is presented at using a constant turn-on angle and applying variation for the turn-off angle. The torque per current increases from θ_{off} = 64^o until 68^o and decreases from θ_{off} = 70^o until 74^o. But this is not standard case for variation of the turn-off angle. Also, as shown in Figure 18 increase the retarding of the turn-off angle, this leads to an increase in the motor speed.

In order to the motor phases respond to continuous drawing of a current from the source, there is a maximum allowable range of θ_{on} and θ_{off} for 3-ph 6/4 SRM. The motor average characteristics values for this range will be stored in the following tables. These characteristics obtained at steady state speed by applying a rated source voltage of 220V.

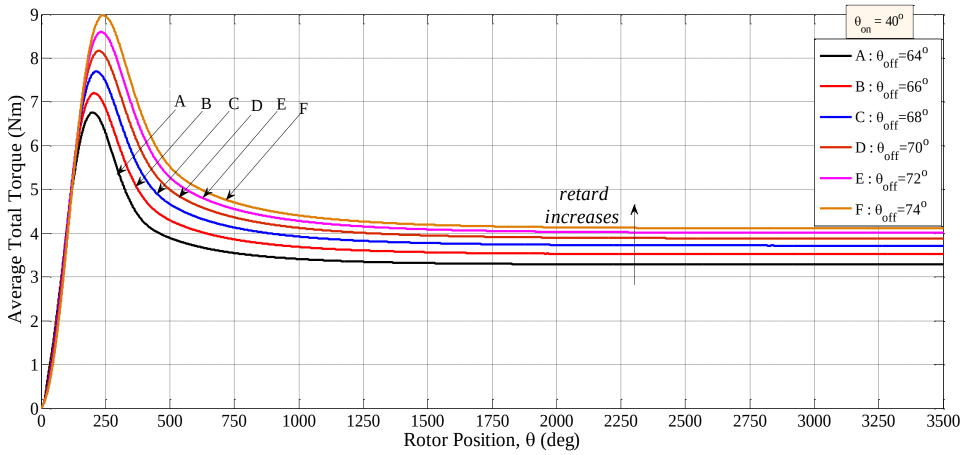

Figure 16. Average total torque versus rotor position for retard turn-off

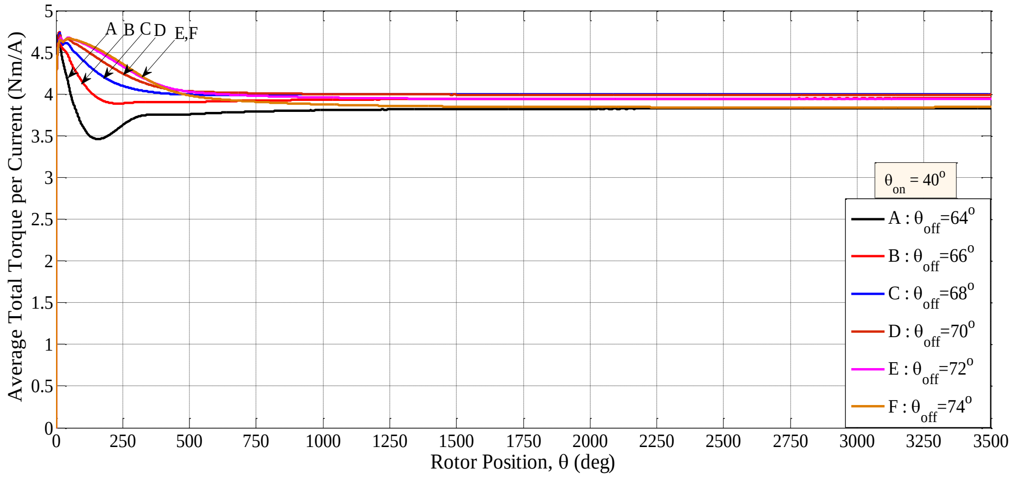

Figure 17. Average total torque per ampere versus rotor position for retard turn-off

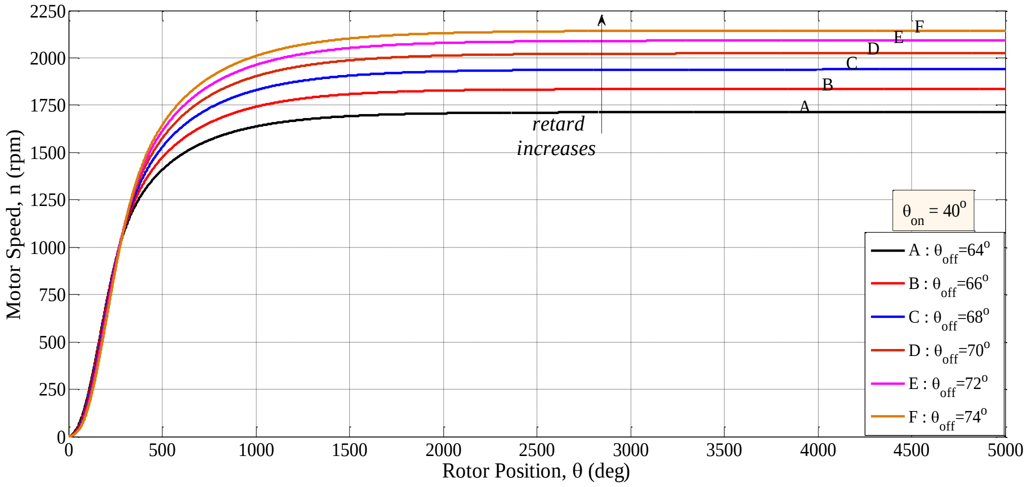

Figure 18. Motor speed versus rotor position for retard turn-off

The average source current is shown in Table 1 at different values of turn-on and turn-off angles to obtain the optimum performance ch/s for the drive system at no-load; where the minimum allowable limit and the maximum allowable limit of the switching angles are presented. From Table 1 adjustment of the switching angles (turn-on angle of 60^o and turn-off angle of 64^o) is presented in order to get a minimum average source current of 0.107A (at using the asymmetric bridge converter equals 0.152A) [36]. But in Table 2 the maximum average total torque is 4.552Nm at turn-on angle of 36^o and turn-off angle of 80^o (at using the asymmetric bridge converter equals 2.224Nm) [36]. But this value of the torque not present optimum machine performance because the optimum performance depends on the maximum torque per current is 6.016Nm/A at turn-on angle of 60^o and turn-off angle of 68^o (at using the asymmetric bridge converter equals 2.224Nm) [36] as presented in Table 3. The motor speed at all switching angles is presented in Table 4.

Table 1. The Average source current of proposed converter in (Ampere)

θ_{off} / θ_{on}	64°	66°	68°	70°	72°	74°	76°	78°	80°	82°	84°	86°	88°	90°
36°	1.090	1.120	1.156	1.199	1.247	1.301	1.361	1.428	1.501	1.582	1.672	1.773	1.885	2.013
38°	0.970	1.002	1.039	1.081	1.128	1.181	1.238	1.302	1.373	1.451	1.537	1.633	1.742	1.865
40°	0.857	0.891	0.929	0.971	1.017	1.067	1.124	1.187	1.255	1.330	1.413	1.507	1.613	1.733
42°	0.753	0.787	0.826	0.868	0.914	0.964	1.019	1.080	1.146	1.220	1.301	1.393	1.496	1.615
44°	0.656	0.692	0.730	0.773	0.818	0.868	0.922	0.981	1.046	1.118	1.198	1.288	1.390	1.508
46°	0.566	0.603	0.643	0.684	0.730	0.779	0.832	0.890	0.954	1.025	1.104	1.193	1.294	1.411
48°	0.485	0.522	0.562	0.603	0.648	0.696	0.748	0.806	0.869	0.939	1.016	1.105	1.205	1.322
50°	0.409	0.448	0.487	0.529	0.573	0.620	0.672	0.729	0.790	0.859	0.936	1.023	1.123	1.240
52°	0.339	0.379	0.419	0.460	0.504	0.550	0.600	0.656	0.717	0.785	0.861	0.948	1.048	1.165
54°	0.276	0.316	0.356	0.397	0.440	0.485	0.535	0.589	0.650	0.716	0.791	0.877	0.977	1.095
56°	0.216	0.257	0.297	0.338	0.380	0.424	0.474	0.527	0.586	0.652	0.726	0.811	0.911	1.030
58°	0.160	0.201	0.243	0.283	0.323	0.368	0.416	0.469	0.526	0.591	0.664	0.748	0.848	0.968
60°	0.107	0.149	0.191	0.231	0.272	0.315	0.362	0.413	0.469	0.534	0.605	0.689	0.789	0.910

Table 2. The Average total torque of proposed converter in (Newton.meter)

θ_{off} / θ_{on}	64°	66°	68°	70°	72°	74°	76°	78°	80°	82°	84°	86°	88°	90°
36°	3.608	3.845	4.042	4.202	4.328	4.424	4.492	4.534	4.552	4.545	4.517	4.465	4.392	4.297
38°	3.457	3.693	3.889	4.049	4.177	4.275	4.344	4.387	4.406	4.401	4.373	4.323	4.250	4.155
40°	3.283	3.518	3.716	3.878	4.008	4.109	4.181	4.226	4.247	4.244	4.218	4.169	4.098	4.003
42°	3.084	3.321	3.521	3.687	3.821	3.925	4.000	4.049	4.073	4.073	4.049	4.003	3.933	3.841
44°	2.862	3.101	3.305	3.476	3.615	3.724	3.804	3.857	3.885	3.888	3.868	3.824	3.757	3.667
46°	2.617	2.860	3.070	3.247	3.392	3.506	3.592	3.651	3.684	3.692	3.676	3.635	3.571	3.483
48°	2.355	2.603	2.819	3.003	3.156	3.277	3.369	3.434	3.473	3.485	3.473	3.437	3.376	3.289
50°	2.080	2.333	2.555	2.748	2.908	3.037	3.138	3.209	3.253	3.272	3.265	3.231	3.174	3.090
52°	1.792	2.050	2.284	2.484	2.652	2.791	2.899	2.978	3.029	3.053	3.051	3.024	2.969	2.888
54°	1.500	1.763	2.002	2.212	2.393	2.540	2.657	2.744	2.803	2.834	2.838	2.814	2.764	2.687
56°	1.204	1.475	1.720	1.940	2.127	2.287	2.413	2.509	2.576	2.613	2.624	2.606	2.560	2.486
58°	0.909	1.182	1.435	1.661	1.862	2.031	2.168	2.273	2.350	2.395	2.412	2.400	2.359	2.289
60°	0.613	0.889	1.151	1.385	1.596	1.775	1.923	2.039	2.124	2.177	2.202	2.198	2.162	2.094

Table 3. The Average total torque per mpere of proposed converter in (Newton.meter/Ampere)

θ_{off} / θ_{on}	64°	66°	68°	70°	72°	74°	76°	78°	80°	82°	84°	86°	88°	90°
36°	3.309	3.432	3.494	3.504	3.470	3.400	3.300	3.176	3.032	2.873	2.700	2.519	2.330	2.135
38°	3.564	3.687	3.744	3.746	3.703	3.621	3.508	3.369	3.210	3.035	2.846	2.647	2.440	2.228
40°	3.829	3.949	4.002	3.996	3.940	3.849	3.720	3.561	3.385	3.191	2.984	2.766	2.541	2.310
42°	4.100	4.217	4.264	4.248	4.181	4.070	3.926	3.750	3.553	3.339	3.112	2.874	2.629	2.379
44°	4.366	4.484	4.525	4.499	4.418	4.290	4.127	3.931	3.713	3.477	3.228	2.969	2.702	2.433
46°	4.624	4.742	4.778	4.745	4.649	4.503	4.321	4.102	3.862	3.603	3.330	3.048	2.760	2.469
48°	4.863	4.985	5.021	4.977	4.868	4.706	4.503	4.261	3.997	3.713	3.418	3.111	2.801	2.489
50°	5.082	5.209	5.246	5.196	5.075	4.895	4.672	4.407	4.118	3.810	3.488	3.158	2.825	2.492
52°	5.274	5.411	5.452	5.398	5.267	5.070	4.827	4.538	4.225	3.891	3.545	3.191	2.834	2.480
54°	5.447	5.587	5.632	5.580	5.442	5.232	4.968	4.656	4.318	3.958	3.586	3.208	2.829	2.453
56°	5.580	5.760	5.788	5.743	5.599	5.390	5.095	4.759	4.396	4.011	3.615	3.211	2.809	2.414
58°	5.680	5.884	5.920	5.877	5.754	5.518	5.208	4.851	4.472	4.053	3.635	3.207	2.781	2.364
60°	5.717	5.973	6.016	5.987	5.868	5.631	5.314	4.935	4.525	4.081	3.640	3.187	2.739	2.303

Table 4. The Average motor speed of proposed converter in (revolution per minute)

θ_{off} / θ_{on}	64°	66°	68°	70°	72°	74°	76°	78°	80°	82°	84°	86°	88°	90°
36°	1883	2006	2109	2192	2259	2309	2344	2366	2375	2372	2357	2330	2292	2242
38°	1804	1927	2029	2113	2180	2231	2267	2289	2299	2297	2282	2256	2218	2168
40°	1713	1836	1939	2024	2091	2144	2181	2205	2216	2215	2201	2175	2138	2089
42°	1609	1733	1837	1924	1994	2048	2087	2113	2125	2125	2113	2089	2053	2004
44°	1493	1618	1725	1814	1886	1943	1985	2013	2027	2029	2018	1996	1961	1914
46°	1366	1492	1602	1694	1770	1830	1875	1905	1922	1927	1918	1897	1863	1817
48°	1229	1358	1471	1567	1647	1710	1758	1792	1812	1819	1812	1793	1761	1716
50°	1085	1217	1334	1434	1518	1585	1637	1675	1698	1707	1703	1686	1656	1613
52°	936	1070	1191	1296	1384	1456	1513	1554	1581	1593	1592	1578	1549	1507
54°	783	921	1045	1155	1248	1325	1386	1432	1462	1479	1481	1468	1442	1402
56°	629	769	897	1012	1110	1193	1259	1309	1344	1364	1369	1360	1336	1297
58°	474	617	748	867	972	1060	1131	1186	1226	1250	1259	1253	1231	1194
60°	320	465	600	723	832	926	1003	1064	1108	1137	1149	1147	1128	1093

5. CONCLUSIONS

At steady state; for a constant value of θ_{off}; if the advancing of θ_{on} increases (i.e, decreasing the value of θ_{on}), then: the average source current, average total torque and motor speed are directly proportional to advance of the θ_{on}. The average total torque per current is inversely proportional to advance of the θ_{on}. At steady state; for a constant value of θ_{on}; if the retarding/delaying of θ_{off} increases (i.e, increasing value of θ_{off}), then: the average source current, average total torque and motor speed are directly proportional to retard of θ_{off}. The average total torque per current is inversely proportional to retard of θ_{off}. At steady state, for a constant switching angles: the average source current is inversely proportional to increase of source voltage. The average total torque, average total torque per current and the motor speed are directly proportional to increase of source voltage.

APPENDIX

DC voltage rating	: U	= 220 V
Stator phase resistance	: R	= 17 Ω
Aligned inductance	: L_{al}	= 0.605 H
Unaligned inductance	: L_{ul}	= 0.155 H
Viscous friction coefficient	: B	= 0.0183 N.m.Sec^2
Rated speed	: n_r	= 1000 rpm
Rated phase current	: I_r	= 3 A
Rated torque	: T_e	= 1 Nm
Inertia constant	: J	= 0.0013 Kg.m^2

REFERENCES

[1] S. Vukosavic and V. R. Stefanovic, "SR Motor Inverter Topologies: A Comparative Evaluation," *IEEE Transactions IAS*, Vol. 27, No. 6, pp. 1034–1047, November/December 1991.

[2] A. Hava, V. Blasko, and T. A. Lipo, "A Modified C-Dump Converter For Variable Reluctance Machines," *Industry Applications, IEEE Transactions on Power Electronics*, Vol. 28, Issue 5, pp. 1017–1022, September/October 1992.

[3] S. Park and T. A. Lipo, "New Series Resonant Converter For Variable Reluctance Motor Drive," *Record of 23rd Annual IEEE Power Electronics Specialists Conference*, pp. 833–838, 29 June–3 July 1992, Toledo, Spain.

[4] P. Vijayragbvan and R. Krishnan, "Front-End Buck Converter Topology for SRM Drives – Design and Control," *29th Annual Conference of IEEE Industrial Electronics Society*, pp. 3013–3018, Vol. 3, 2–6 November 2003, Blacksburg, USA.

[5] B. K. Bose, T. J. E. Miller, P. M. Szczesny, and W. H. Bicknell, "Microcomputer Control of Switched Reluctance Motor," *IEEE Transactions Industrial Application*, pp. 708–715, Vol. 22, No. 4, July/August 1986.

[6] D. A. Torrey and J. H. Lang, "Optimal-Efficiency Excitation Of Variable Reluctance Motor Drives," *IEE Electronic Power Applications*, pp. 1–14, Vol. 138, No. 1, January 1991.

[7] T. J. E. Miller, "Switched Reluctance Motor Drives And Their Control," Magna Physics Publishing, Hillsboro, OH; and Oxford Science Publications, Oxford, U.K, 1993.

[8] R. Krishnan, "Switched Reluctance Motor Drives: Modeling, Simulation, Analysis, Design, and Applications," CRC Press, 2001.

[9] Christos Mademlis and Iordanis Kioskeridis, "Performance Optimization in Switched Reluctance Motor Drives With Online Commutation Angle Control," *IEEE Transactions On Energy Conversion*, pp. 448–457, Vol. 18, No. 3, September 2003.

[10] J. Kim, K. Ha, and R. Krishnan, "Single-Controllable-Switch-Based Switched Reluctance Motor Drive for Low Cost, Variable-Speed Applications," *IEEE Transactions on Power Electronics*, pp. 379–387, Vol. 27, No. 1, January 2012.
[11] T. W. Ching, K. T. Chau, and C. C. Chan, "A Novel Zero-Voltage Soft-Switching Converter For Switched Reluctance Motor Drives," *24th IEEE Annual Conference on Industrial Electronics Society*, pp. 899–904, Vol. 2, 31 August–4 September 1998, Aachen, Germany.
[12] M. Ilic-Spong, T. J. E. Miller, S. R. MacMinn, and J. S. Thorp, "Instantaneous Torque Control Of Electric Motor Drives," *IEEE Transactions on Power Electronics*, pp. 55–61, Vol. 2, No. 1, January 1987.
[13] R. S. Wallace and D. G. Taylor, "A Balanced Commutator For Switched Reluctance Motors To Reduce Torque Ripple," *IEEE Transactions on Power Electronics*, pp. 617–626, Vol. 7, No. 4, October 199.
[14] C. H. Kim and I. J. Ha, "A New Approach To Feedback Linearizing Control Of Variable Reluctance Motors For Direct Drive Applications," *IEEE Transactions on Control Systems Technology*, pp. 348–362, Vol. 4, No. 4, July 1996.
[15] M. Rodrigues, P. J. C. Branco, and W. Suemitsu, "Fuzzy Logic Torque Ripple By Turn-Off Angle Compensation For Switched Reluctance Motors," *IEEE Transactions on Industry Electronics*, pp. 711–714, Vol. 48, Issue 3, June 2001.
[16] M. T. Lamchich, "Torque Control," InTech Publisher, 2011.
[17] K. Srivastava et al., "Simulation And Modeling of 8/6 Switched Reluctance Motor Using Digital Controller," *International Journal of Electronics Engineering*, pp. 241–246, Vol. 3, No. 2, 2011.
[18] Y. Sozer et al., "Automatic Control Of Excitation Parameters For Switched Reluctance Motor Drives," *IEEE Transactions on Power Electronics*, pp. 594–603, Vol. 18, Issue 2, March 2003.
[19] C. S. Dragu and R. Belmans, "Optimal Firing Angles Control For Four-Quadrant Operation of an 8/6 SRM," *Proceedings of 10th European Conference on Power Electronics and Applications*, pp. 1–10, Toulouse, France, 2–4 September 2003.
[20] C. Mademlis and I. Kioskeridis, "Performance Optimization in Switched Reluctance Motor Drives with Online Commutation Angle Control," *IEEE Transactions on Energy Conversion*, pp. 448–457, Vol. 18, September 2003.
[21] Emad S. Abdel-Aliem, "Speed Control of Switched Reluctance Motors in Aircraft Applications," Scholar's Press, 2015.
[22] T. Wichert, "Design and Construction Modifications of Switched Reluctance Machines," *Ph.D Thesis, Warsaw University of Technology*, 2008.
[23] K. Ha, "Position Estimation In Switched Reluctance Motor Drives Using The First Switching Harmonics Of Phase Voltage And Current," *Ph.D Dissertation, Faculty of the Virginia Polytechnic Institute and State University*, Blacksburg, Virginia, June 2008.
[24] W. Lu, "Modeling And Control Of Switched Reluctance Machines for Electro-Mechanical Brake Systems," Ph.*D Dissertation, Graduate School of the Ohio State University*, 2005.
[25] H. E. Akhter et al., "Determination Of Optimum Switching Angles For Speed Control Of Switched Reluctance Motor Drive System," *Indian Journal of Engineering and Materials Sciences*, pp. 151–168, Vol. 11, June 2004.
[26] William Shepherd and Li Zhang, "Power Converter Circuits," Marcel Dekker, Inc, 2004.
[27] Hans-Dieter Stölting, Eberhard Kallenbach and Wolfgang Amrhein, "Handbook of Fractional-Horsepower Drives," Springer, 2006.
[28] Mukhtar Ahmad, "High Performance AC Drives: Modelling, Analysis and Control," Springer, 2010.
[29] Rik De Doncker, Duco W.J. Pulle and André Veltman, "Advanced Electrical Drives: Analysis, Modeling, Control," Springer, 2011.
[30] H. G. Vasquez, "Variable Speed Control Of A Switched Reluctance Motor In A Heat Pump Application," *Ph.D Dissertation, Graduate School of the University of Alabama, Department of Mechanical Engineering*, Tuscaloosa, Alabama, USA, 2003.
[31] T. J. E. Miller, "Brushless Permanent-Magnet and Reluctance Motor Drives," Clarendon Press, Oxford, 1989.
[32] Timothy L. Skvarenina, "The Power Electronics Hand Book," CRC Press, 2002.
[33] Muhammad H. Rashid, "Power Electronics Handbook," Academic Press, 2001.
[34] Bin Wu, "High-Power Converters and AC Drives," IEEE Press, John Wiley & Sons, Inc., 2006.
[35] Samia M. Mahmoud, Mohsen Z. El-Sherif, Emad S. Abdel-Aliem, and Maged N. F. Nashed, "Studying Different Types Of Power Converters Fed Switched Reluctance Motor," *International Journal of Electronics and Electrical Engineering*, pp. 281-290, Vol. 1, No. 4, December 2013.
[36] Maged N. F. Nashed, Samia M. Mahmoud, Mohsen Z. El-Sherif, and Emad S. Abdel-Aliem, "Optimum Change Of Switching Angles On Switched Reluctance Motor Performance," *International Journal of Current Engineering and Technology*, pp. 1052-1057, Vol. 4, No. 2, April 2014.
[37] P. Srinivas and K. Amulya, "Comparative Analysis of DITC Based Switched Reluctance Motor Using Asymmetric Converter and Four-Level Converter," *Bulletin of Electrical Engineering and Informatics*, pp. 109-119, Vol. 5, No. 1, March 2016.
[38] Maged N. F. Nashed, Samia M. Mahmoud, Mohsen Z. El-Sherif, and Emad S. Abdel-Aliem, "Hysteresis Current Control of Switched Reluctance Motor in Aircraft Applications," *International Journal of Power Electronics and Drive Systems (IJPEDS)*, pp. 376-392, Vol. 4, No. 3, September 2014.